Supporting Information

for

Monitoring the adsorption of per- and polyfluoroalkyl substances on carbon black by LDI-MS capable of simultaneous analysis of elemental and organic carbon

Ke Min[ab], Shenxi Deng[a], Zhao Shu[a], Yong Li[ac], Bo Chen[b], Ming Ma[b], Qian Liu[ad*] and Guibin Jiang[a]

[a]State Key Laboratory of Environmental Chemistry and Ecotoxicology, Research Center for Eco-Environmental Sciences, Chinese Academy of Sciences, Beijing 100085, China

[b]Key Laboratory of Phytochemical R&D of Hunan Province, Ministry of Education Key Laboratory of Chemical Biology & Traditional Chinese Medicine Research, Hunan Normal University, Changsha 410081, China

[c]National Engineering Laboratory for Applied Forest Ecological Technology in Southern China, Faculty of Life Science and Technology, Central South University of Forestry and Technology, Changsha 410004, China

[d]Taishan Institute for Ecology and Environment (TIEE), Jinan 250100, China

*Corresponding authors. Email: qianliu@rcees.ac.cn

Table of contents

1. Experimental section for SI

Extraction of soot from real $PM_{2.5}$ samples

Soot-containing $PM_{2.5}$ samples were collected in Shijiazhuang, Hebei Province, China in heavy haze weather during November 16-17, 2020. The extraction procedures of soot from real $PM_{2.5}$ samples referred to a previously reported study as follows:[1] first, an appropriate volume of 5 M KOH solution was mixed with the sample and heated for 12 h at 95 ℃, and then the supernatant was discarded after centrifugation at 10000 rpm for 20 min to remove silicon dioxide. The residue was washed two times with deionized water and then mixed with HCl (3 M) to remove carbonate grains and metallic oxides. The supernatant was discarded by centrifugation, and the residue was washed again. After that, the residue was mixed with *n*-hexane/acetone (1:1 v/v), followed by ultrasonication for 10 min, and collected by centrifugation. This step was repeated twice to obtain the final soot particles.

Characterization of extracted soot and CB standard

In order to verify the homogeneity of extracted soot from environmental samples and carbon black (CB) standard, we investigated their MS spectra, morphology, elemental fingerprints, and particle size range. First, we tested blank solvent (deionized water), soot, and CB standard by LDI-MS. As shown in Fig. S1a, the MS spectra of the blank solvent were quite clean with no MS signal background interference. While, the soot and CB standard (see Fig. S1b and 1c) both showed a series of characteristic carbon cluster peaks (C_3^--C_{10}^-) with repeated mass units ($\Delta m/z$ 12 u) between m/z 20-600 with the highest intensity at C_6^- (m/z 72). Importantly, soot and CB standard produced highly consistent characteristic MS peaks, i.e., the serial carbon cluster peaks, with the similar peak intensity ratios (see heat maps in Fig. S1b and 1c). Then, the particle morphology and elemental distribution of soot and CB standard were characterized by SEM and EDS, respectively. Fig. S1d and 1e shows that soot and CB standard both had a near spherical appearance, and their elemental compositions were generally consistent (e.g., C, O, Na, Si, Cl, and K), with C (mass ratio > 60%) and Si (from the silicon slice) being the dominant elements. Finally, the particle size distribution of soot and CB standard was obtained by nanoparticle tracking analyzer (NTA) (see Fig. S1f). It can be seen that their particle size distributions were close and relatively narrow (the particle size was less than 200 nm). Overall, the results mentioned above demonstrated that the extracted soot and CB standard had the same MS fingerprints, similar morphology and size distribution.

Preparation of mixed CB and different OC standard solutions

We selected typical organic compounds (OCs) that are ubiquitous in environmental media including an industrial adhesive (bisphenol S, BPS), an organochlorine pesticide (pentachlorophenol, PCP), an endocrine disrupter estradiol (E2) and two nitropolycyclic aromatic hydrocarbon aromatic hydrocarbons (1-nitropyrene and 9-nitroanthracene). BPS was purchased from AccuStandard (New Haven, CT, USA). PCP and E2 were purchased from Dr. Ehrenstorfer (Augsburg, Germany). 1-Nitropyrene was purchased from Aladdin (Shanghai, China). 9-Nitroanthracene was purchased from Sigma (St. Louis, MO, USA). All standard solutions were prepared in 50% methanol, and stock standards were BPS (0.1 mg mL^{-1}), PCP (1 mg mL^{-1}), E2 (1 mg mL^{-1}), 1-nitropyrene (1 mg mL^{-1}) and 9-nitroanthracene (1 mg mL^{-1}). Then, an appropriate amount of CB was added to these OC standard solution to prepare four mixed standard solutions, i.e., BPS/CB mixed standard solution (BPS 100 ng mL^{-1}, CB 0.2 mg mL^{-1}), PCP/CB mixed standard solution (PCP 100 ng mL^{-1}, CB 0.2 mg mL^{-1}), E2/CB mixed standard solution (E2 100 ng mL^{-1}, CB 0.2 mg mL^{-1}), 1-nitropyrene/9-nitroanthracene /CB mixed standard solution (1-nitropyrene 100 ng mL^{-1}, 9-nitroanthracene 100 ng mL^{-1}, CB 0.2 mg mL^{-1}). These solutions were ultrasonicated for 5 min prior to analysis. Finally, 1 μL of the mixed standard solution was dropped onto the MALDI target plate and dried prior to LDI-MS measurements.

Validation of the LDI-MS method by Q-TOF-MS

To validate the reliability of method, quantification of PFOS and PFOA were carried out by LDI-MS and Q-TOF-MS, respectively. Regarding LDI-MS, a series of standard working solutions (1.0 uL of each) were dropped on a MALDI target plate, and then allowed to air dry prior to analysis. Scheme of workflow for quantification analysis was presented in Fig. S3a, *m/z* 499 and *m/z* 331 were selected as target ions of PFOS and PFOA, and the calibration curves were constructed by plotting the peak intensity (Y) of target ion to the concentration (X) of target compounds. Calibration curves of PFOS (0.4 to 100 ng mL^{-1}) and PFOA (0.4 to 100 ng mL^{-1}) obtained by LDI-MS are listed in Fig. S4a and 4b, and Table S2. From the calibration curves, an excellent linearity was observed (R^2 was both greater than 0.99). The shot-to shot (n = 20) RSDs obtained under the concentration of 60 ng mL^{-1} were 19.4% for PFOS and 18.3% for PFOA. The sample-to-sample (n = 15) RSDs obtained under the concentration of 60 ng mL^{-1} were 23.1% for PFOS and 23.0% for PFOA. The precision was

satisfactory for LDI-MS measurements. Next, to validate the established LDI-MS method, PFOS and PFOA were also quantified by Q-TOF-MS (see Fig. S3b and Fig. S4c), and all the aqueous solutions were filtered through a 0.22 μm filter membranes prior to analysis, and quantitative analysis was performed using extracted ion chromatograms (EIC), such as *m/z* 499 for PFOS, and *m/z* 369 for PFOA, were recorded in full-scan mode. The scheme of workflow for quantification analysis was presented in Fig. S3b, and the calibration curves were constructed by plotting the peak area (*Y*) of extracted target ion versus the concentration of target compound (*X*). The calibration curves of PFOS (0.4 to 100 ng mL^{-1}) and PFOA (0.4 to 100 ng mL^{-1}) obtained by Q-TOF-MS are listed in Fig. S4d and 4e, and Table S2, showing an excellent linear relationship and precision (for PFOS, R^2 = 0.9933, RSD = 0.5-2.5%; for PFOA, R^2 = 0.9929, RSD = 0.2-2.7%).

Then, we quantified the residual PFOS and PFOA in the sample solutions after CB adsorption by both LDI-MS and Q-TOF-MS. Taking PFOS (100 ng mL^{-1}) and PFOA (100 ng mL^{-1}) as target compounds, different CB mass (0.02, 0.05, 0.1 and 0.2 mg mL^{-1}) was applied in adsorption for 5 min to obtain a pre-equilibrium state, and then the sample solutions were collected by membrane filtration. The residual PFOS and PFOA in the final sample solutions were quantified and compared by LDI-MS and Q-TOF-MS. The results are presented in Fig. S4f and Table S3, and an excellent consistency was obtained between the residual concentrations of PFOS and PFOA determined by these two techniques (R > 0.98). This result demonstrated that the quantitative results with LDI-MS were highly accurate and reliable.

2. Supporting figures

Fig. S1 MS fingerprinting, morphology, and particle size of extracted soot and CB standard. MS spectra of (a) blank solvent, (b) soot, and (c) CB standard obtained by LDI-MS, with the heat maps showing the ratios of characteristic fingerprint peaks of soot (C_3^--C_{10}^-). The particle morphology and elemental fingerprints of (d) soot and (e) CB standard obtained by SEM and EDS. (f) The particle sizes of soot and CB standard obtained by NTA.

Fig. S2 The Scheme of workflow for quantification of PFOS and PFOA by (a) LDI-MS and (b) Q-TOF-MS method.

Fig. S3 Calibration curves of (a) PFOS and (b) PFOA obtained by LDI-MS. (c) The typical MS spectra of PFOS and PFOA obtained by Q-TOF-MS. Calibration curves of (d) PFOS and (e) PFOA obtained by Q-TOF-MS. (f) Comparison of the concentration of PFOS and PFOA determined by using LDI-MS and Q-TOF-MS.

Fig. S4 Simultaneous analysis of EC and multiple types of OCs by LDI-MS under the positive ion mode. The typical MS spectra of (a) pyrene and dimethyl-benzo-anthracene, TTAB, DDBAC and TDBAC, (b) nicotine and cotinine mixed with CB standard.

Fig. S5 LDI-MS spectra for monitoring the adsorption of PFOS on CB. The sample solutions were collected at regular adsorption time intervals (1, 5, 20, 40, 60, 120 and 180 min) without membrane filtration.

Fig. S6 LDI-MS spectra for monitoring the adsorption of PFOS on CB. The sample solutions were sampled at regular adsorption time intervals (1, 5, 20, 40, 60, 120 and 180 min), and filtered through a 0.22 μm filter membrane.

Fig. S7 LDI-MS spectra of CB and PFOS with pre- and post-membrane filtration.

Fig. S8 MS spectra of PFOS in the absence and presence of surfactants with different adsorption time.

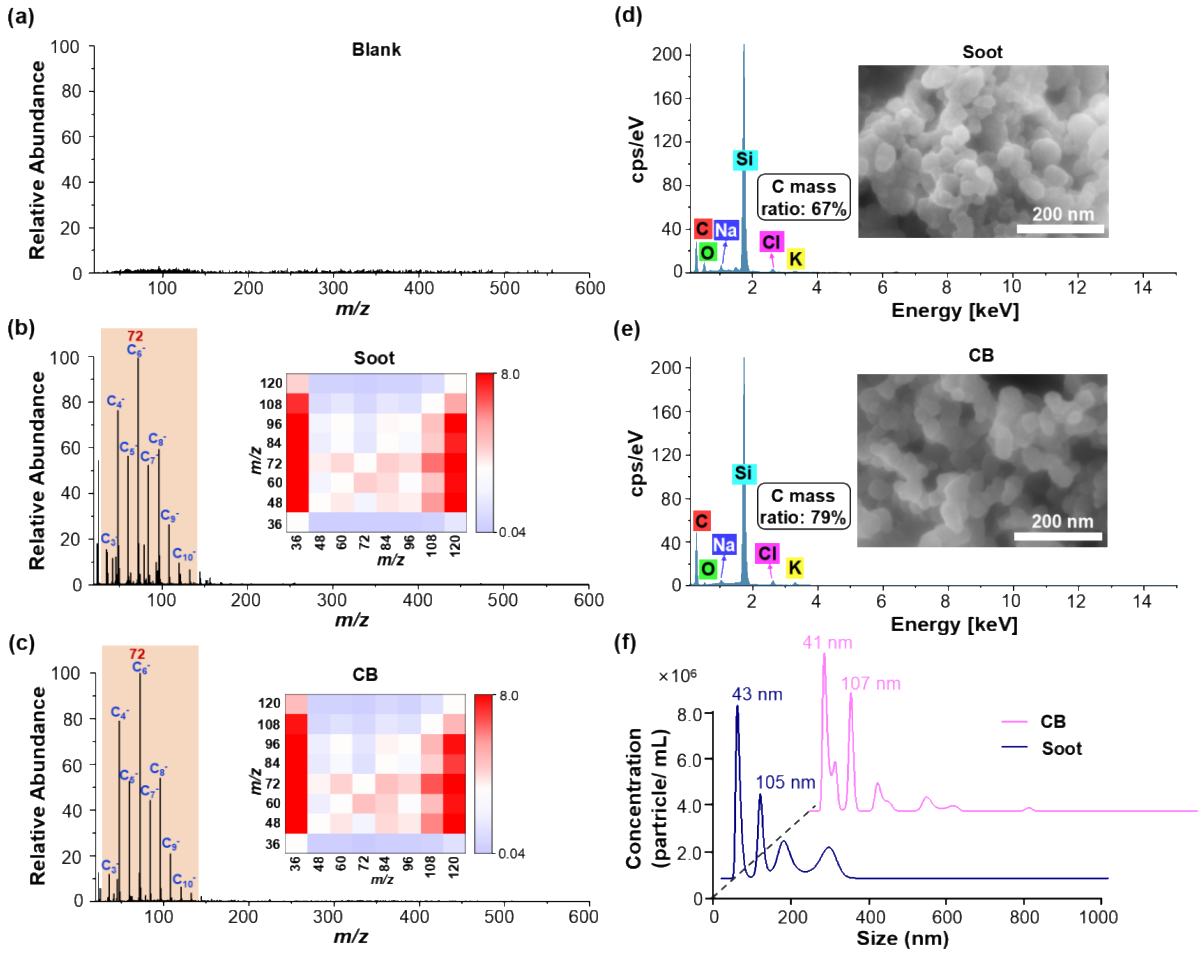

Fig. S1 MS fingerprinting, morphology, and particle size of extracted soot and CB standard. MS spectra of (a) blank solvent, (b) soot, and (c) CB standard obtained by LDI-MS, with the heat maps showing the ratios of characteristic fingerprint peaks of soot (C_3^--C_{10}^-). The particle morphology and elemental fingerprints of (d) soot and (e) CB standard obtained by SEM and EDS. (f) The particle sizes of soot and CB standard obtained by NTA. *Note:* C_3^- (*m/z* 36), C_4^- (*m/z* 48), C_5^- (*m/z* 60), C_6^- (*m/z* 72), C_7^- (*m/z* 84), C_8^- (*m/z* 96), C_9^- (*m/z* 108) and C_{10}^- (*m/z* 120).

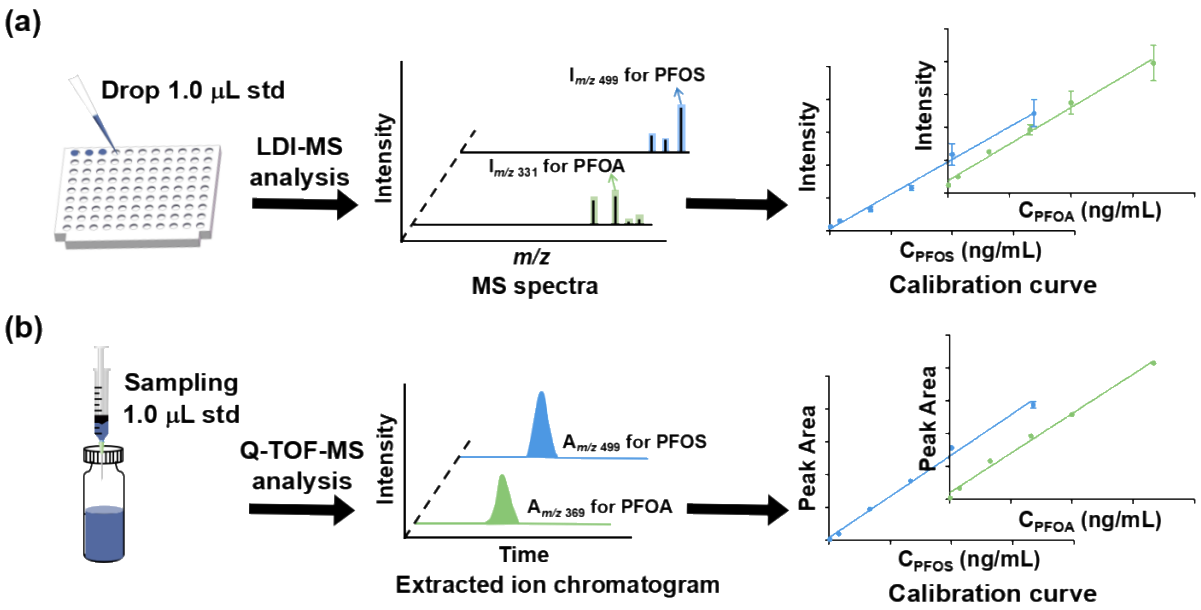

Fig. S2 The Scheme of workflow for quantification of PFOS and PFOA by (a) LDI-MS and (b) Q-TOF-MS method. *Note:* $I_{m/z\ 499}$ and $I_{m/z\ 331}$ refer to the MS signal intensities of target ions of PFOS and PFOA in LDI-MS. $A_{m/z\ 499}$ and $A_{m/z\ 369}$ refer to the peak areas of extracted target ions of PFOS and PFOA in Q-TOF-MS.

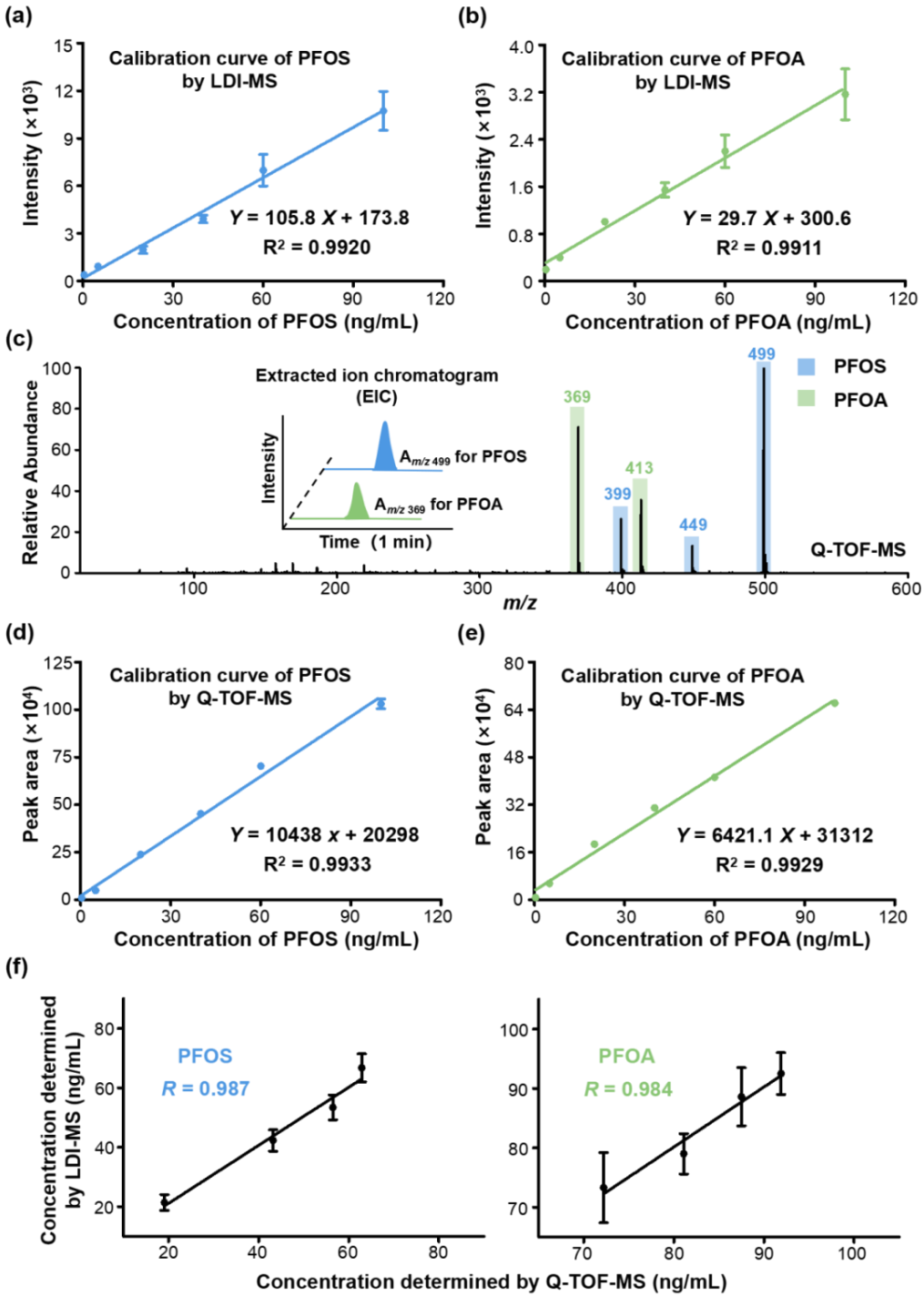

Fig. S3 Calibration curves of (a) PFOS and (b) PFOA obtained by LDI-MS. (c) The typical MS spectra of PFOS and PFOA obtained by Q-TOF-MS. Calibration curves of (d) PFOS and (e) PFOA obtained by Q-TOF-MS. (f) Comparison of the concentration of PFOS and PFOA determined by using LDI-MS and Q-TOF-MS.

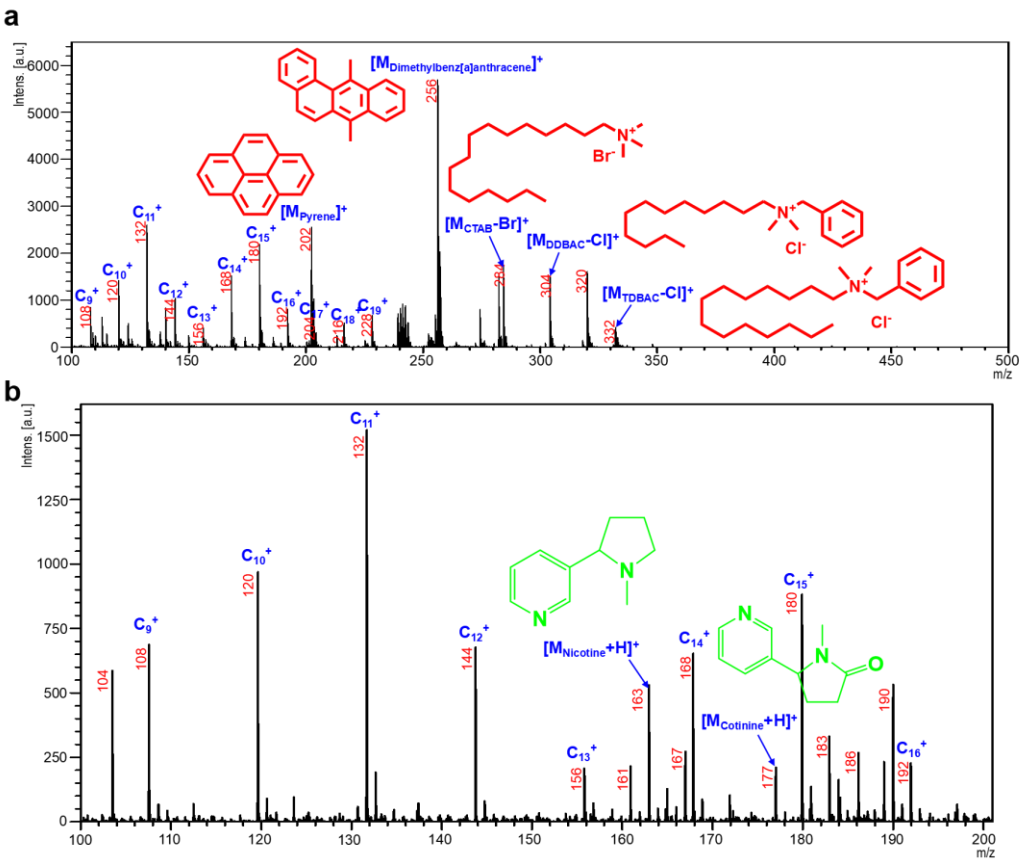

Fig. S4 Simultaneous analysis of EC and multiple types of OCs by LDI-MS under the positive ion mode. The typical MS spectra of (a) pyrene and dimethyl-benzo-anthracene, TTAB, DDBAC and TDBAC, (b) nicotine and cotinine mixed with CB standard.

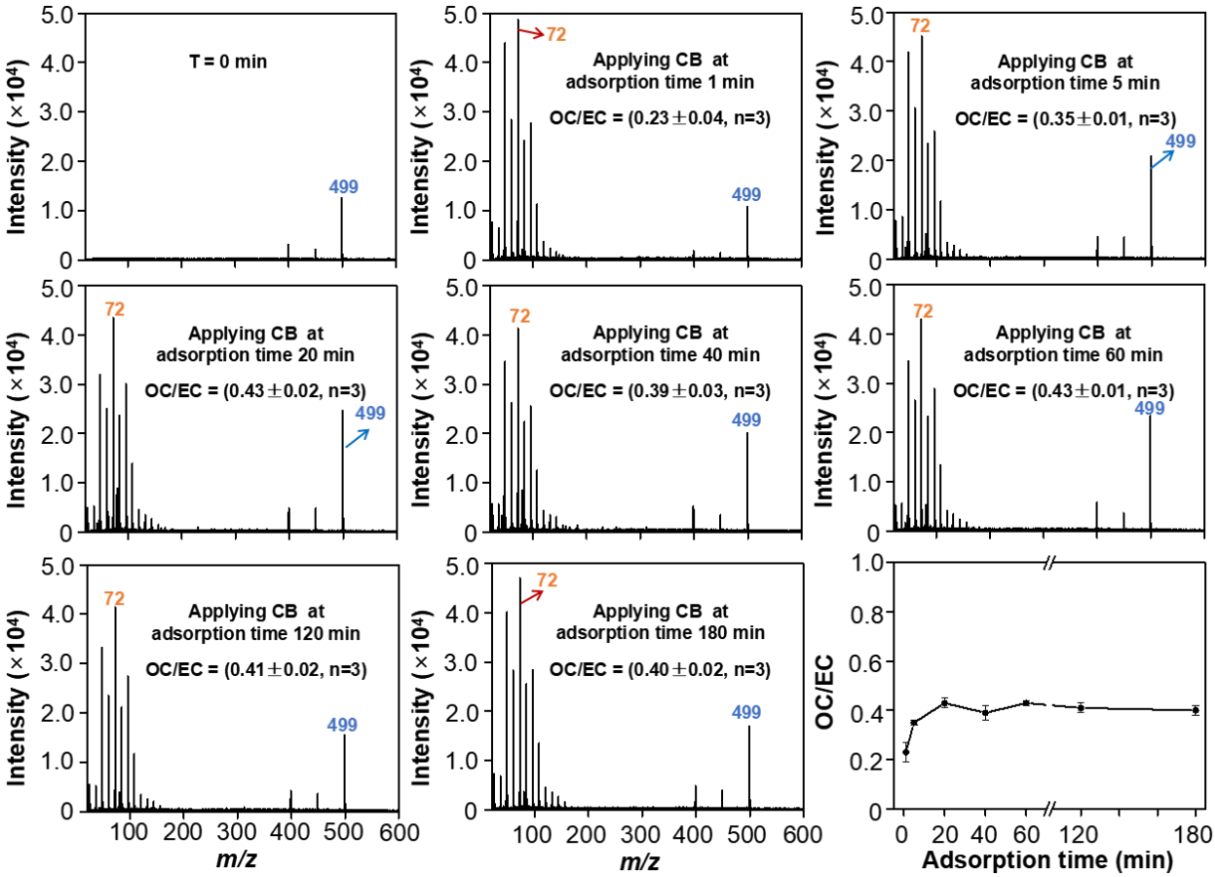

Fig. S5 LDI-MS spectra for monitoring the adsorption of PFOS on CB. The sample solutions were collected at regular adsorption time intervals (1, 5, 20, 40, 60, 120 and 180 min) without membrane filtration. *Note:* CB and PFOS were used as models of EC and OC, respectively. The value of OC/EC refers to the ratio of the MS signal intensity ($I_{m/z\ 499}/I_{m/z\ 72}$).

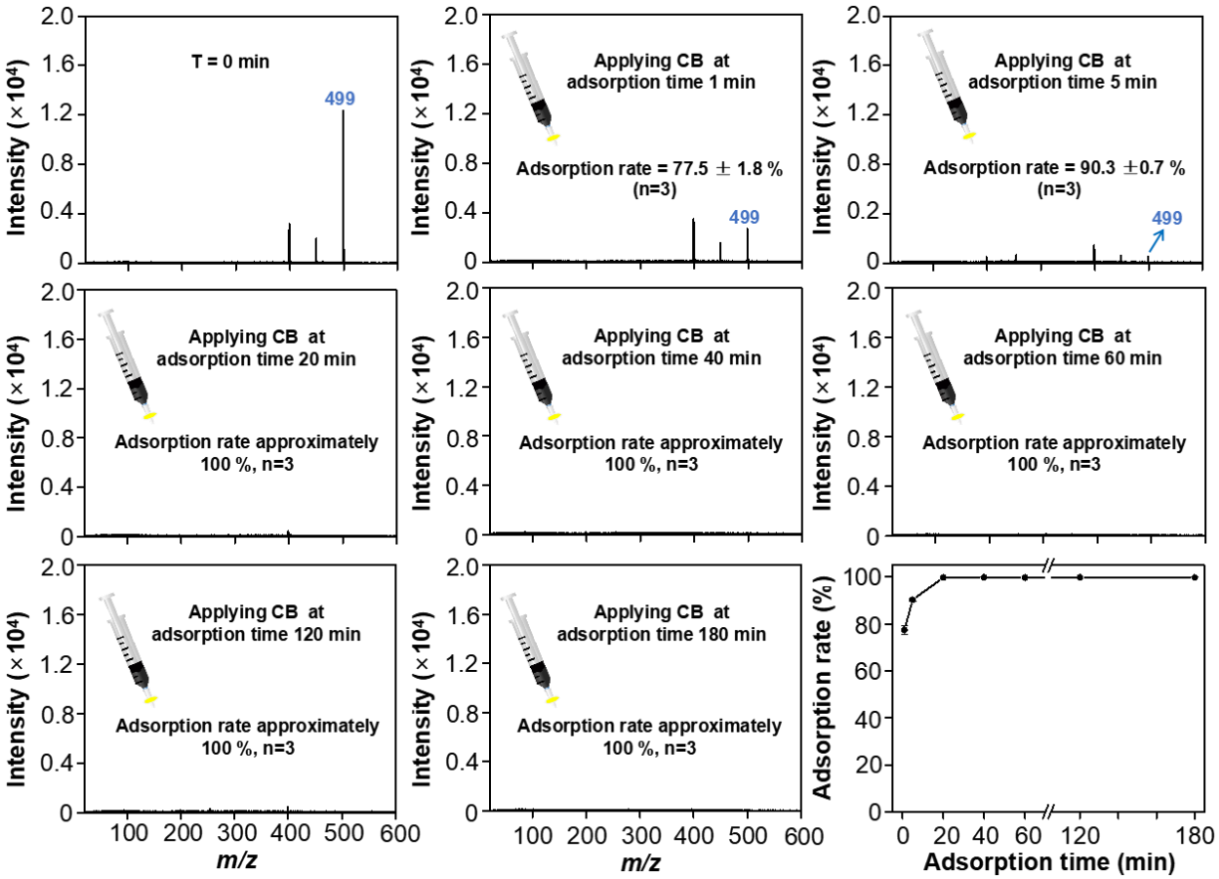

Fig. S6 LDI-MS spectra for monitoring the adsorption of PFOS on CB. The sample solutions were sampled at regular adsorption time intervals (1, 5, 20, 40, 60, 120 and 180 min), and filtered through a 0.22 μm filter membrane. *Note:* CB and PFOS were used as models of EC and OC, respectively. The adsorption rate (%) was calculated by the percentage of the signal intensity difference of OC before and after adsorption to the signal intensity value before adsorption.

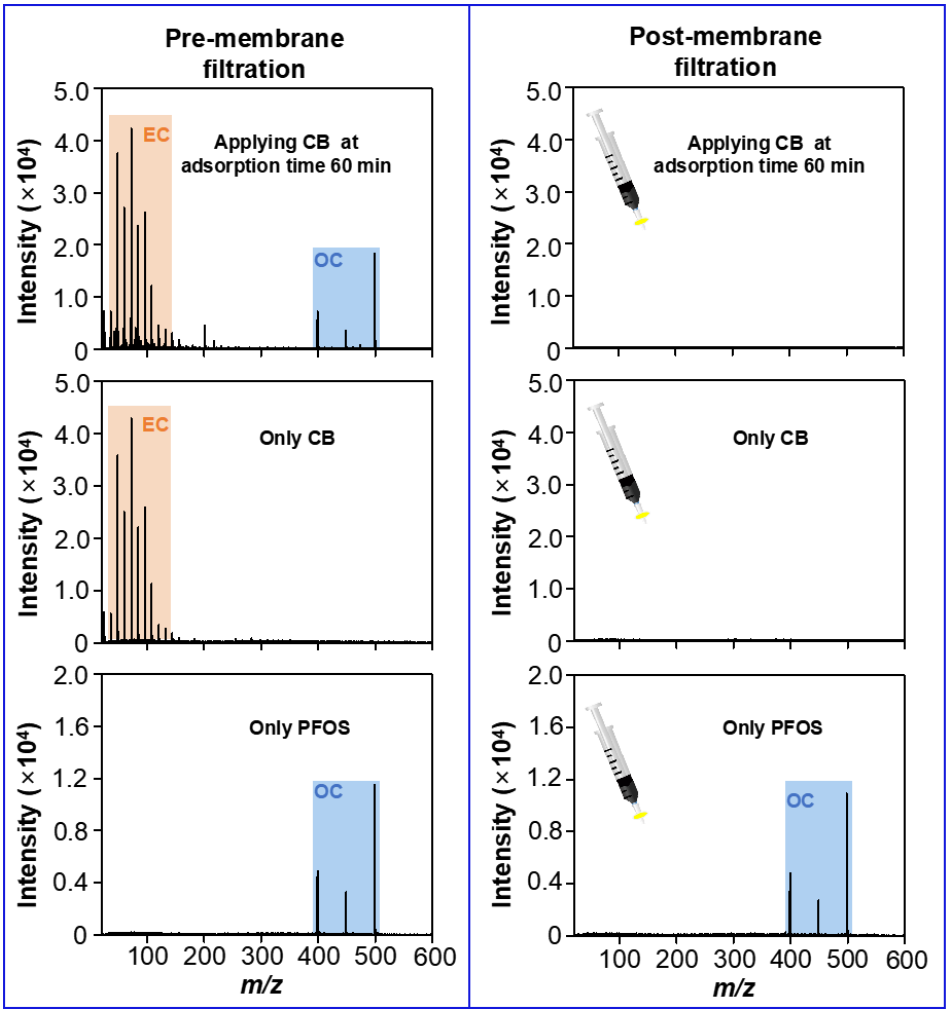

Fig. S7 LDI-MS spectra of CB and PFOS with pre- and post-membrane filtration. *Note:* CB and PFOS were used as models of EC and OC, respectively.

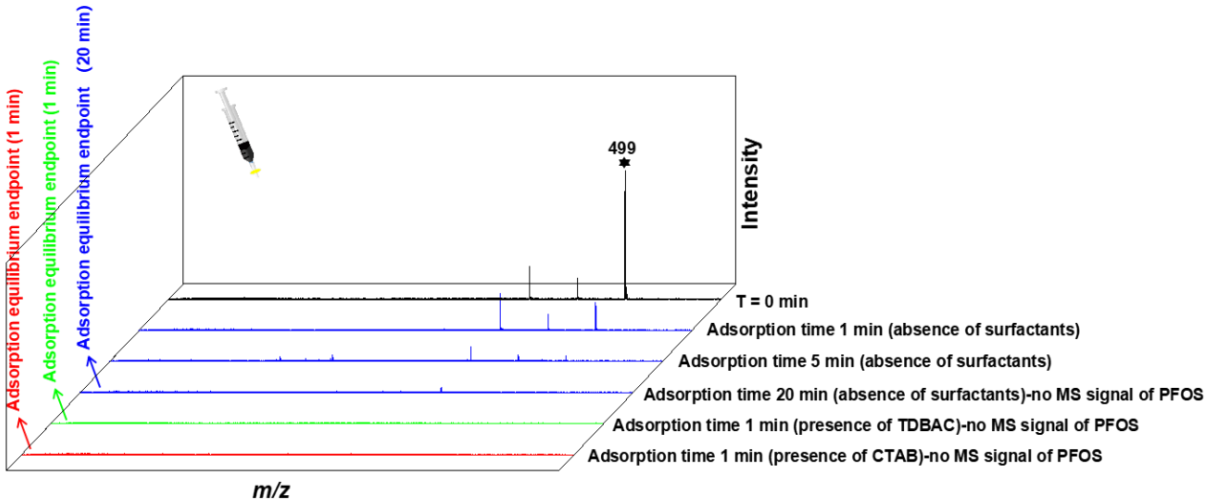

Fig. S8 MS spectra of PFOS in the absence and presence of surfactants with different adsorption time.

Note: m/z 499 was selected as the characteristic ion for PFOS.

3. Supporting tables

Table S1. The characteristic MS peaks of elemental carbon (EC) and multiple types of organic carbons (OCs) obtained by LDI-MS.

Table S2. Calibration curves of PFOS and PFOA were obtained by LDI-MS and Q-TOF-MS. All calibration points obtained by LDI-MS were performed in three parallel spots (average of 15 shots data for each spot), and all calibration points from Q-TOF-MS were repeated in triplicate (n = 3).

Table S3. Quantitative results of residual PFOS and PFOA in sample solutions, which were adsorbed by applying different CB mass (0.02, 0.05, 0.1 and 0.2 mg mL^{-1}) for adsorption time 5 min, obtained by LDI-MS and Q-TOF-MS. Error values are standard deviations (n = 15 for LDI-MS and n = 3 for Q-TOF-MS).

Table S1. The characteristic MS peaks of elemental carbon (EC) and multiple types of organic carbons (OCs) obtained by LDI-MS.

Compound	Characteristic peaks (*m/z*)	Corresponding ionization structure
CB	36, 48, 60, 72, 84, 96, 108, 120	C_3^--C_{10}^-
PFOS	399, 449, 499	$[M_{PFOS}-C_2F_4-H]^-$, $[M_{PFOS}-CF_2-H]^-$, $[M_{PFOS}-H]^-$
PFOA	281, 331, 369, 413	$[M_{PFOA}-CF_4COOH]^-$, $[M_{PFOA}-F_2COOH]^-$, $[M_{PFOA}-COOH]^-$, $[M_{PFOA}-H]^-$
PFNA	331, 381	$[M_{PFNA}-CF_4COOH]^-$, $[M_{PFNA}-F_2COOH]^-$
PFDA	431, 469	$[M_{PFDA}-F_2COOH]^-$, $[M_{PFDA}-COOH]^-$
PFDoA	531, 569	$[M_{PFDoA}-F_2COOH]^-$, $[M_{PFDoA}-COOH]^-$
BPS	157, 249	$[M_{BPS}-C_6H_5O]^-$, $[M_{BPS}-H]^-$
PCP	265	$[M_{PCP}-H]^-$
E2	271	$[M_{E2}-H]^-$
9-nitroanthracene	193	$[M_{9\text{-nitroanthracene}}-NO]^-$
1-nitropyrene	217	$[M_{1\text{-nitropyrene}}-NO]^-$

Note: CB was one key model EC. PFASs (including PFOS, PFOA, PFNA, PFDA and PFDoA), BPS, PCP, E2, 9-nitroanthracene, and 1-nitropyrene were used as representatives of OCs.

Table S2. Calibration curves of PFOS and PFOA obtained by LDI-MS and Q-TOF-MS. All calibration points obtained by LDI-MS were performed in three parallel spots (average of 15 shots data for each spot), and all calibration points from Q-TOF-MS were repeated in triplicate (n = 3).

Method	Compound	Linear range	Calibration curve	R^2	Range of RSD%
LDI-MS	PFOS	0.4-100 ng mL^{-1}	Y = 105.8 X + 173.8	0.9920	6.0-14.3%
	PFOA	0.4-100 ng mL^{-1}	Y = 29.7 X +300.6	0.9911	7.9-13.6%
Q-TOF-MS	PFOS	0.4-100 ng mL^{-1}	Y =10483 X + 20298	0.9933	0.5-2.5%
	PFOA	0.4-100 ng mL^{-1}	Y = 6421.1 X +31312	0.9929	0.2-2.7%

Table S3. Quantitative results of residual PFOS and PFOA in sample solutions, which were adsorbed by applying different CB mass (0.02, 0.05, 0.1 and 0.2 mg mL^{-1}) for adsorption time 5 min, obtained by LDI-MS and Q-TOF-MS. Error values are standard deviations (n = 15 for LDI-MS and n = 3 for Q-TOF-MS).

Sample solution with membrane filtration	Residual concentration (ng/mL)			
	LDI-MS		Q-TOF-MS	
	PFOS	PFOA	PFOS	PFOA
Applying 0.02 mg mL^{-1} ECB	66.7 ± 4.7	92.5 ± 3.5	62.9 ± 1.3	91.9 ± 0.6
Applying 0.05 mg mL^{-1} ECB	53.4 ± 4.2	88.6 ± 4.9	56.5 ± 0.9	87.5 ± 0.7
Applying 0.1 mg mL^{-1} ECB	42.3 ± 3.6	79.0 ± 3.4	43.2 ± 2.5	81.1 ± 0.7
Applying 0.2 mg mL^{-1} ECB	21.4 ± 2.7	73.2 ± 5.9	19.1 ± 1.5	72.2 ± 1.0

Note: The initial concentration of PFOS and PFOA were both 100 ng mL^{-1} before applying CB adsorption.

4. Reference for SI

1 Y. Lin, X. Huang, Y. Liu, D. Cao, D. Lu, Z. Feng, Q. Liu, Z. Lin, G. Jiang, Identification, Quantification, and Imaging of the Biodistribution of Soot Particles by Mass Spectral Fingerprinting, *Anal. Chem.*, 2021, **93**, 6665-6672.